nature genetics

SUPPLEMENTARY INFORMATION

https://doi.org/10.1038/s41588-018-0083-2

In the format provided by the authors and unedited.

Mapping the in vivo fitness landscape of lung adenocarcinoma tumor suppression in mice

Zoë N. Rogers[1,8], Christopher D. McFarland[2,8], Ian P. Winters[1], Jose A. Seoane[1,3,4], Jennifer J. Brady[1], Stephanie Yoon[5], Christina Curtis[1,3,4,6], Dmitri A. Petrov[2*] and Monte M. Winslow[1,4,6,7*]

[1]Department of Genetics, Stanford University School of Medicine, Stanford, CA, USA. [2]Department of Biology, Stanford University, Stanford, CA, USA. [3]Department of Medicine (Oncology), Stanford University School of Medicine, Stanford, CA, USA. [4]Stanford Cancer Institute, Stanford University School of Medicine, Stanford, CA, USA. [5]Department of Biology, Massachusetts Institute of Technology, Cambridge, MA, USA. [6]Cancer Biology Program, Stanford University School of Medicine, Stanford, CA, USA. [7]Department of Pathology, Stanford University School of Medicine, Stanford, CA, USA. 8These authors contributed equally: Zoë N. Rogers, Christopher D. McFarland. *e-mail: dpetrov@stanford.edu; mwinslow@stanford.edu

a

	Kras$^{LSL\text{-}G12D}$	*Kras*$^{LSL\text{-}G12D}$; *p53*$^{flox/flox}$	*Kras*$^{LSL\text{-}G12D}$; *Lkb1*$^{flox/flox}$
p53	Increased tumor burden Shorter survival[Jackson, 2005]	N/A	No Published Data
Lkb1	Increased tumor burden Shorter survival[Ji, 2007]	No Published Data	N/A
Rb1	Slightly increased tumor burden slightly shorter survival[Ho, 2009]	No Published Data	No Published Data
Atm	Possible slight reduction in survival (with *Kras*$^{LSL\text{-}G12V\text{-}ires\text{-}bGeo}$ allele)[Efeyan, 2009]	No Published Data	No Published Data
Cdkn2a	Slightly increased tumor burden Slightly shorter survival[Schuster,2014]	No Published Data	No Published Data
Apc	Increase in tumor burden[Sanchez-Rivera, 2014]	Non-significant increase in tumor burden[Sanchez-Rivera, 2014]	No Published Data
Arid1a	Non-significant increase in tumor burden[Rogers, 2017 and Walter,2017]	Non-significant increase in tumor burden[Walter,2017]	No Published Data
Setd2	Increase in tumor burden[Rogers, 2017 and Walter,2017]	Increase in tumor burden[Walter,2017]	No Published Data
Keap1	No increase in tumor burden[Rogers, 2017]	Increase in tumor burden[Romero, 2017]	No Published Data
Smad4	No increase in tumor burden[Rogers, 2017]	No Published Data	No Published Data
Rbm10	Increase in tumor burden[Rogers, 2017]	No Published Data	No Published Data

b

	TCGA, 2014			GENIE, 2017		
# of Samples (%)	All 230	*TP53*^{mut} 107 (47%)	*LKB1*^{mut} 43 (19%)	All 1563	*TP53*^{mut} 775 (53%)	*LKB1*^{mut} 274 (15%)
P53(TP53)	47%	N/A	30%	50%	N/A	38%
LKB1(STK11)	19%	12%	N/A	18%	13%	N/A
SETD2	9%	7%	2%	7%	6%	5%
RB1	7%	10%	9%	6%	9%	4%
RBM10	9%	7%	17%	5%	5%	5%
APC	4%	5%	7%	6%	6%	7%
CDKN2A	24%	26%	21%	11%	14%	14%
ARID1A	8%	8%	3%	8%	10%	8%
KEAP1	19%	17%	40%	13%	12%	42%
SMAD4	4%	5%	2%	4%	5%	4%
ATM	12%	5%	23%	10%	7%	15%

Supplementary Figure 1

The current state of genetically-engineered mouse models of lung cancer for the analysis of the putative tumor suppressor alterations in this study and the frequency of these genomic alterations in human lung adenocarcinoma.

a. Summary of data from published studies in which the putative tumor suppressor genes studied here were inactivated in the context of oncogenic *Kras*-driven lung cancer models, with or without inactivation of *p53* or *Lkb1*.

b. The percent of tumors with potentially inactivating alterations (frameshift or non-synonymous mutations, or genomic loss) in each tumor suppressor gene for all tumors (All) as well as for tumors with potentially inactivating alterations in *TP53* (*TP53*^{mut}) or *LKB1* (*LKB1*^{mut}). The percent of tumors with each type of alteration is indicated. Data is shown for two clinical cancer genomics studies: The Cancer Genome Atlas (TCGA, 2014)[32], and the Genomics Evidence Neoplasia Information Exchange (GENIE, 2017) database[4].

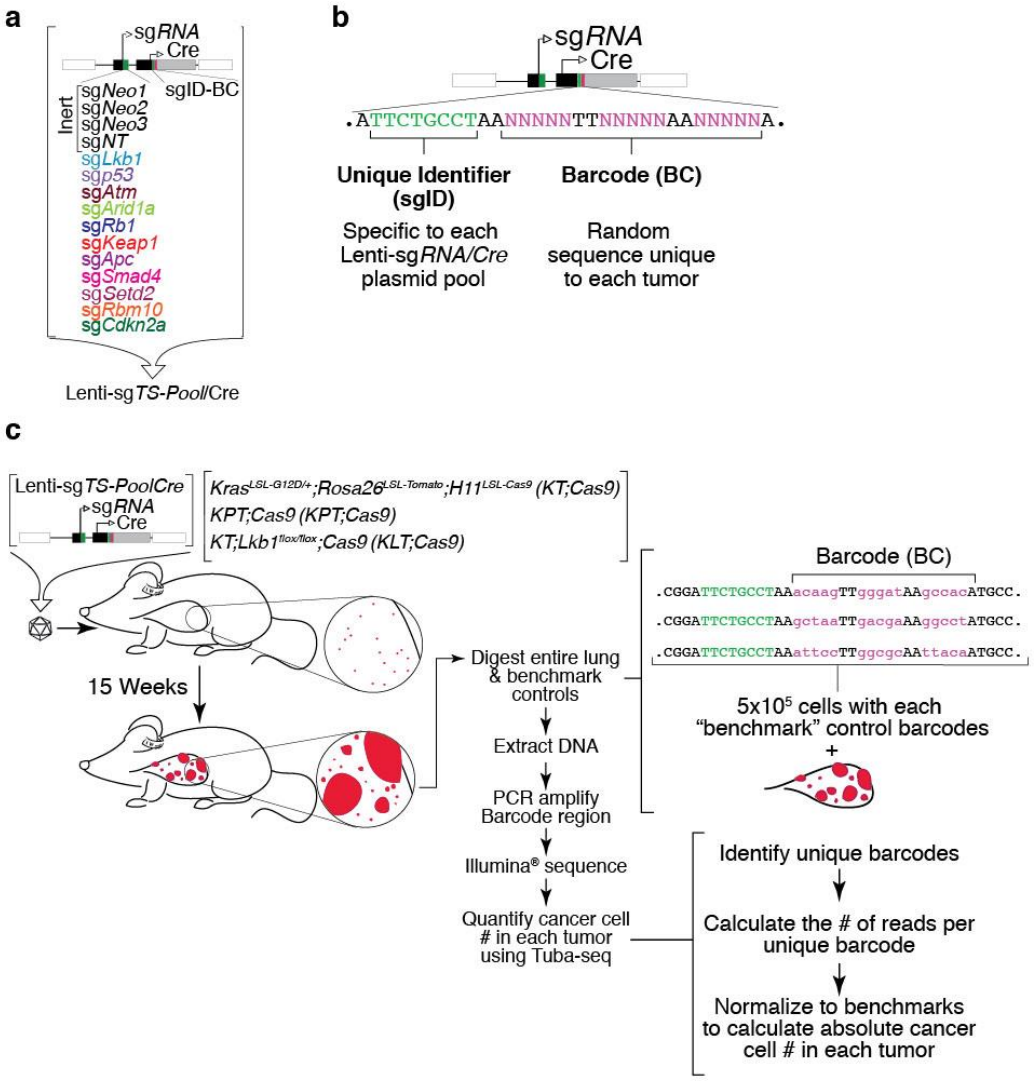

Supplementary Figure 2

Description of multiplexed lentiviral vectors, tumor initiation, and Tuba-seq pipeline to quantify tumor size distributions *in vivo*.

a. Lenti-sg*TS-Pool/Cre* contains four vectors with inert sgRNAs and eleven vectors with tumor suppressor gene targeting sgRNAs. Each sgRNA vector contains a unique sgID and a random barcode. NT = Non-Targeting.

b. Schematic of the sgID-barcode region of the vectors in Lenti-sg*TS-Pool/Cre*. Lenti-sg*TS-Pool/Cre* contains vectors with fifteen different 8-nucleotide unique identifiers (sgIDs) which link a given sgID-barcode read to a specific sgRNA. These vectors also contain a 15-nucleotide random barcode element. This double barcode system allows identification of individual tumors, as well as the sgRNA in the vector that initiates each tumor.

c. Transduction of lung epithelial cells with the barcoded Lenti-sg*TS-Pool/Cre* pool initiates lung tumors in genetically engineered mouse models with (1) a Cre-regulated oncogenic *KrasG12D* (*Kras*$^{LSL\text{-}G12D/+}$) allele, (2) a Cre reporter allele (*Rosa26*$^{LSL\text{-}Tomato}$), (3) a Cre-regulated *Cas9* allele (*H11*$^{LSL\text{-}Cas9}$), as well as (4) homozygous floxed alleles of either *p53* or *Lkb1*. Lentiviral vectors stably integrate into the genome of the transduced cell. Tumors were initiated in *KT;Cas9*, *KPT;Cas9*, and *KLT;Cas9* mice to generate 31 different genotypes of lung tumors. Mice were analyzed after 15 weeks of tumor growth. Genomic DNA was extracted from whole lungs, after the addition of barcoded "benchmark" cell lines, the sgID-barcode region was PCR amplified, deep-sequenced, and analyzed to determine the relative expansion of each uniquely barcoded tumor using the Tuba-seq pipeline.

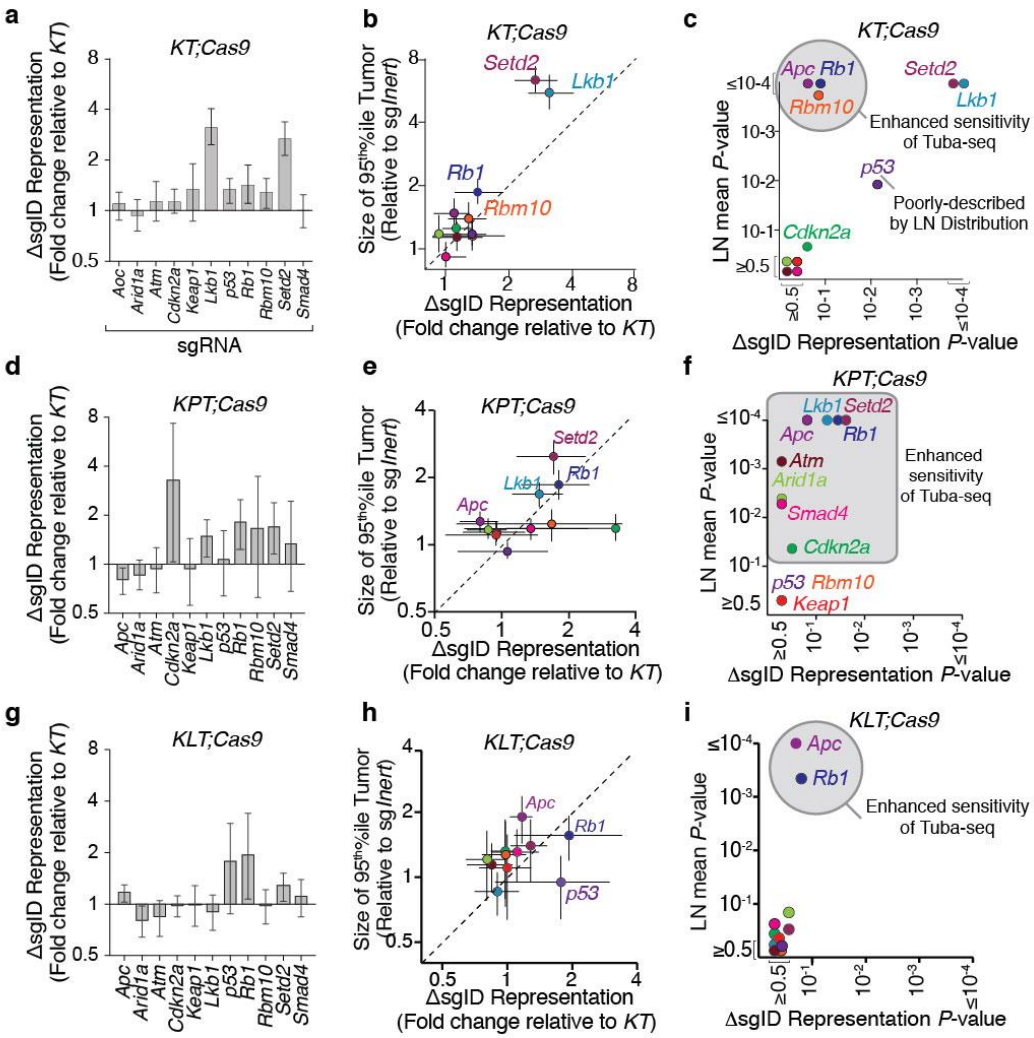

Supplementary Figure 3

Tumor suppression in *Kras*^{G12D}-driven lung adenocarcinoma *in vivo*.

a. Fold change in sgID representation (ΔsgID representation) in *KT;Cas9* mice relative to *KT* mice, which lack *Cas9* and therefore should not expand relative to sg*Inert*. Several sgRNAs (sgIDs) increase in representation, reflecting the increased growth of tumors with inactivation of the targeted tumor suppressor genes. Means and 95% confidence intervals are shown.

b,c. The ability to detect tumor suppressive effects is improved by analyzing individually-barcoded tumors compared to bulk sgRNA representation (ΔsgID representation). (**b**) Analysis of the relative size of the 95th percentile tumor with each sgRNA identifies somewhat similar estimates of relative tumor size as bulk ΔsgID representation, which exhibits wider confidence intervals and generally weaker effect sizes. (**c**) *P*-value of the Log-Normal mean (LN mean) measure of relative tumor size versus *P*-value ΔsgID representation. Because individual tumor sizes are measured and then properly normalized to eliminate exogenous sources of noise, both the 95th percentile and LN Mean metrics identify functional tumor suppressors with greater confidence and precision. *p53* loss is an exception, as its growth effects are poorly described by a Log-Normal distribution. All *P*-values are two-sided and obtained via 2 x 10^6 Bootstrapping permutation tests and a Bonferroni-correction for the number of investigated tumor suppressors.

d-f. Same as in **a-c**, except for growth effects in *KPT;Cas9* mice. Fold change is relative to *KT* mice, while 95th percentile and LN Mean size estimates are relative to *KPT;Cas9* internal sg*Inert* controls.

g-i. Same as in **a-c**, except for growth effects in *KLT;Cas9* mice. No tumor suppressors would have been identified without Tuba-seq.

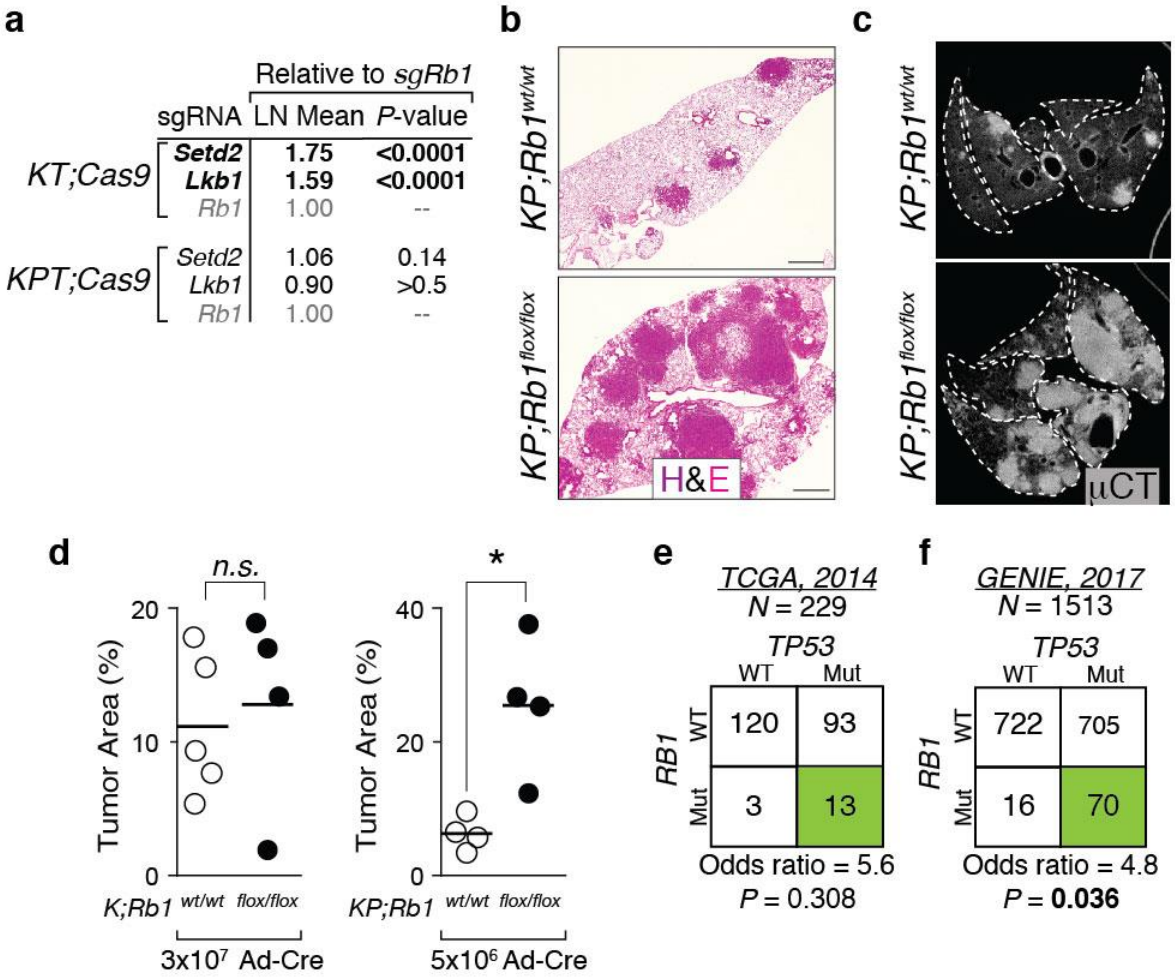

Supplementary Figure 4

Rb and p53 tumor suppressor cooperativity in lung adenocarcinoma identified by Tuba-seq, confirmed in a mouse model using Cre/lox regulated alleles, and supported by the co-occurrence of RB1 and TP53 mutations in human lung adenocarcinoma.

a. Relative LN Mean size of sg*Setd2*, sg*Lkb1* and sg*Rb1* tumors. *Rb1* inactivation increase tumor size less that *Setd2* or *Lkb1* inactivation in the *p53*-proficient *KT;Cas9* background. Conversely, *Rb1* inactivation increases tumor size to a similar extent as *Setd2* or *Lkb1* inactivation in the *p53*-deficient *KPT;Cas9* background. *P*-values test null hypothesis of similar LN Mean to sg*Rb1*. $P < 0.05$ in bold.

b. H&E staining of representative lung lobes from *KP* and *KP;Rb1*$^{flox/flox}$ mice with tumors initiated with Adeno-*CMV/Cre*. Mice were analyzed 12 weeks after tumor initiation. Scale bars = 500 µm.

c. Representative *ex vivo* µCT images of the lungs from *KP* and *KP;Rb1*$^{flox/flox}$ mice are shown. Lung lobes are outlined with a dashed white line.

d. Quantification of percent tumor area in *K;Rb1*$^{wt/wt}$, *K;Rb1*$^{flox/flox}$, *KP;Rb1*$^{wt/wt}$, and *KP;Rb1*$^{flox/flox}$ mice. Histological quantification confirms that *Rb1*-deletion increases tumor burden more dramatically in p53-deficient tumors. * *P*-value < 0.05, n.s. = not significant. Titer of *Ad-Cre* is indicated.

e,f. Co-occurrence of *RB1* and *TP53* mutations in two human lung adenocarcinoma genomics datasets: (**e**) TCGA 2014 dataset, and (**f**) the GENIE consortium 2017. *P*-values were calculated using the DISCOVER statistical independence test for somatic alterations (**Methods**)[13]. Combined data from these datasets is shown in **Figure 1g**.

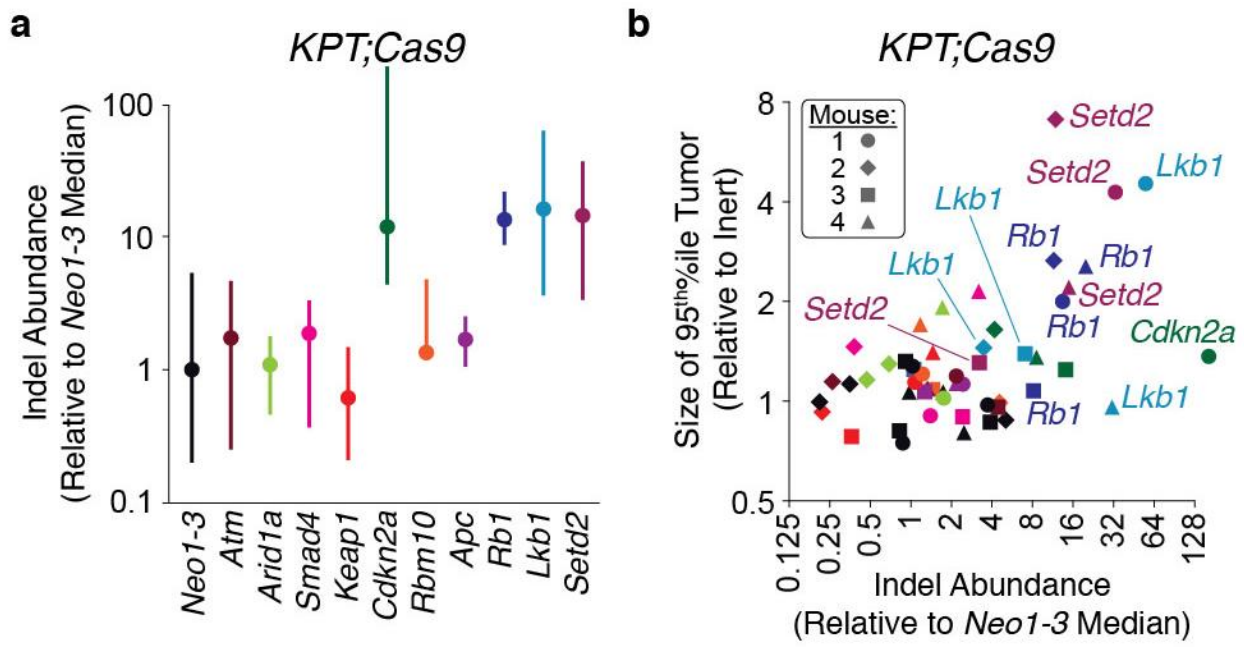

Supplementary Figure 5

Deep sequencing of targeted genomic loci confirms creation of indels at all targeted loci and shows selective expansion of cancer cells with indels in the strongest tumor suppressor genes.

a. Indel abundance in each region targeted by sgRNAs, as determined by deep sequencing of total lung DNA from the targeted regions of four *KPT;Cas9* mice. Indel abundance is normalized to the median abundance of sg*Neo1*, sg*Neo2*, and sg*Neo3*. Error bars denote range of abundances observed, while dots denote median. Indels were observed in all targeted regions. sg*p53* is not shown, as its target site is deleted by *Cre*-mediated recombination of the $p53^{floxed}$ alleles.

b. Indel abundance as described in (**a**) versus the 95th percentile tumor size determined by Tuba-seq (as described in **Fig. 1d**). Each dot represents a single sgRNA in an individual mouse and each mouse is represented by a unique shape. Indel abundance correlated with Tuba-seq size profiles (as expected), however indel abundance does not measure individual tumor sizes and exhibits greater statistical noise. The largest single tumor in this entire analysis, as determined by Tuba-seq, was an sg*Cdkn2a* tumor that similarly appeared as an outlier in the indel analysis—further corroborating faithful analysis of genetic events by Tuba-seq.

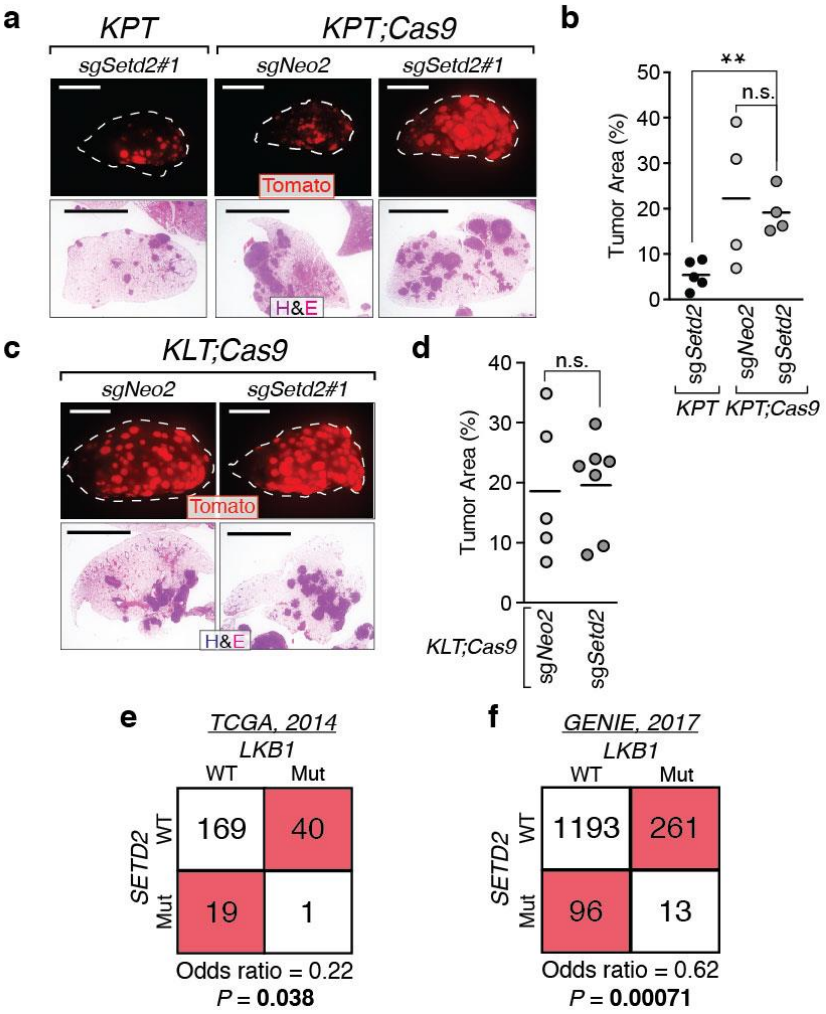

Supplementary Figure 6

Validation of the redundancy between *Setd2* and *Lkb1* in mouse models and in human lung adenocarcinomas.

a. Fluorescence dissecting scope images (**top**) and H&E stained section (**bottom**) of lung lobes from *KPT* and *KPT;Cas9* mice with Lenti-sg*Setd2#1/Cre* or Lenti-sg*Neo2/Cre* initiated tumors. Mice were analyzed after 9 weeks of tumor growth. Lung lobes are outlined with a white dashed line in fluorescence dissecting scope images. Top scale bars = 5 mm. Bottom scale bars = 4 mm.

b. Quantification of percent tumor area in *KPT;Cas9* mice with Lenti-sg*Setd2#1/Cre* or Lenti-sg*Neo2/Cre* initiated tumors, and *KPT* mice with Lenti-sg*Setd2#1/Cre* initiated tumors. Each dot represents a mouse and horizontal bars are the mean. There is an increase in tumor area between *KPT;Cas9* and *KPT* mice with tumors initiated with the same virus, but no difference between *KPT;Cas9* mice tumors initiated with Lenti-sg*Setd2#1/Cre* and those initiated with Lenti-sg*Neo2/Cre*, presumably due to high mouse-to-mouse variability. Because these lentiviral vectors were barcoded, we performed Tuba-seq analysis of these mice to quantify the size of induced tumors (shown in **Figure 2**). sg*Setd2* increased tumor sizes in *KPT;Cas9* relative to sg*Neo2*. ** $P < 0.01$, n.s. is not significant.

c,d. Same as **a,b** except for *KLT;Cas9* mice with Lenti-sg*Setd2#1/Cre* or Lenti-sg*Neo2/Cre* initiated tumors. Mice were analyzed after 9 weeks of tumor growth. Top scale bars = 5 mm. Bottom scale bars = 4 mm. Tuba-seq analysis is shown in **Figure 2**.

e,f. The co-occurrence of *SETD2* and *LKB1* (HGNC name *STK11*) in two human lung adenocarcinoma genomics datasets: (**e**) TCGA 2014 dataset[32] (N = 229 patients), and (**f**) the GENIE Consortium[4] (N = 1563 patients). Two-sided *P*-values were calculated using the DISCOVER statistical independence test. Combined data from these datasets is shown in **Figure 2**.

a

Background Mutation	Co-occurring Mutation	GENIE OR*	GENIE P-value	TCGA OR	TCGA P-value	Combined OR	Combined P-value	LN Mean Ratio raw	LN Mean Ratio weighted
LKB1 (STK11)	*APC*	1.28	0.8633	0.56	0.7747	1.20	0.9379	1.21	1.35
	ARID1A	1.04	**0.9761**	0.69	0.8258	1.00	**0.9798**	1.12	1.20
	ATM	1.85	0.4653	5.19	0.0554	2.13	0.1201	1.04	1.06
	CDKN2A	1.35	0.8796	1.29	0.6800	1.35	0.9055	1.11	1.17
	KEAP1	10.24	**0.0000**	2.84	0.2062	8.29	**0.0000**	1.13	1.20
	RB1	0.60	**0.9990**	1.06	0.7042	0.67	0.9509	1.03	1.05
	RBM10	1.00	0.9586	3.02	0.2429	1.28	0.5722	1.01	1.02
	SETD2	0.62	**0.9996**	0.22	**0.9807**	0.55	**0.9998**	0.73	0.64
	SMAD4	0.97	0.9546	0.65	0.7262	0.94	0.9472	1.12	1.18
	TP53	0.55	**1.0000**	0.41	**0.9979**	0.53	1.0000	1.00	1.00
TP53	*APC*	1.07	0.9312	0.93	0.6906	1.06	0.9270	0.89	0.93
	ARID1A	1.69	0.5613	1.02	0.7275	1.60	0.7741	0.97	1.03
	ATM	0.49	**1.0000**	0.24	**0.9972**	0.46	**1.0000**	1.04	1.10
	CDKN2A	1.70	0.5559	1.64	0.5411	1.69	0.6622	0.97	1.02
	KEAP1	0.93	**0.9971**	0.71	**0.9641**	0.88	**0.9992**	0.93	0.95
	RB1	4.79	**0.0179**	5.59	0.1544	4.88	**0.0190**	1.05	1.11
	RBM10	0.97	0.9550	0.51	**0.9537**	0.85	**0.9959**	0.93	0.89
	SETD2	0.76	**0.9977**	0.76	0.8762	0.75	**0.9917**	0.93	0.75
	SMAD4	1.22	0.8290	1.17	0.6005	1.22	0.8451	0.98	1.05
	LKB1	0.55	**1.0000**	0.41	**0.9979**	0.53	**1.0000**	0.93	0.71

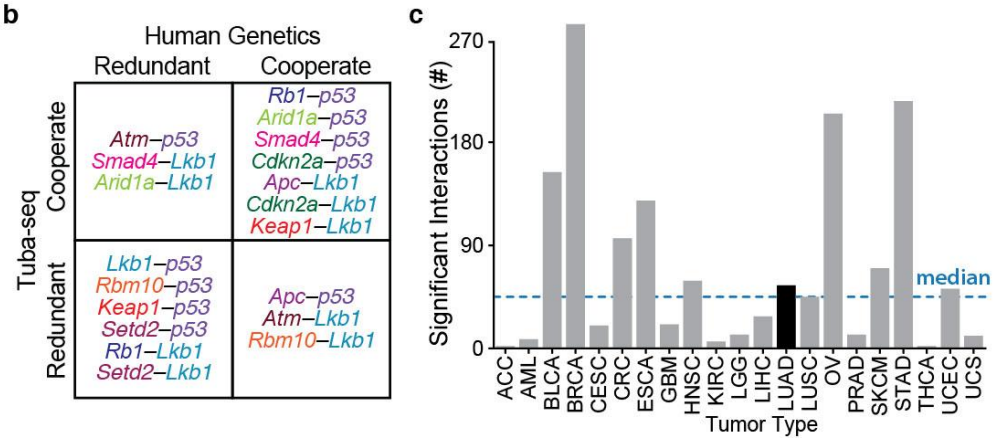

Supplementary Figure 7

Correspondence of Tuba-seq fitness measurements to human genomic patterns.

a. Relative fitness measurements and human co-occurrence rates of the nineteen pairwise interactions that we investigated. LN Mean Ratio is the ratio of relative LN Mean (sg*TS*/sg*Inert*) within the background of interest divided by the mean relative LN mean of all three backgrounds. Background rate can be either an unweighted average of the three backgrounds (raw), or weighted by each background's rate of occurrence in human lung adenocarcinoma (weighted). *OR = "Odds Ratio" of the co-occurrence rate of a gene pair within the human data. One-sided *P*-values of human co-occurrence rates (>0.5 suggest mutual exclusivity) were determined using the DISCOVER test. Combined *P*-values generated using Stouffer's Method (Methods). $P < 0.025$ and $P > 0.975$ are in bold. Fitness measurements and co-occurrence rates generally correspond (Spearman's r = 0.50, *P*-value = 0.03 for weighted LN Mean Ratio; r = 0.4 for unweighted).

b. Graphical summary of fitness measurements and co-occurrence rates from **a**. Human Genetics Cooperativity is defined as a Combined Odds Ratio >1 and Redundant if <1. Tuba-seq Cooperativity is defined as a LN Mean Ratio >1 and Redundant if <1.

c. Number of statistically-significant genetic interactions suggested from a pan-cancer analysis of twenty-one tumor types[3]. Tumor types abbreviations are borrowed from TCGA. Lung adenocarcinoma (LUAD) is black and is predicted to contain a quantity of genetic interactions that is similar to the median, suggesting that the ruggedness of the fitness landscape studied here may be representative of cancer evolution in general.

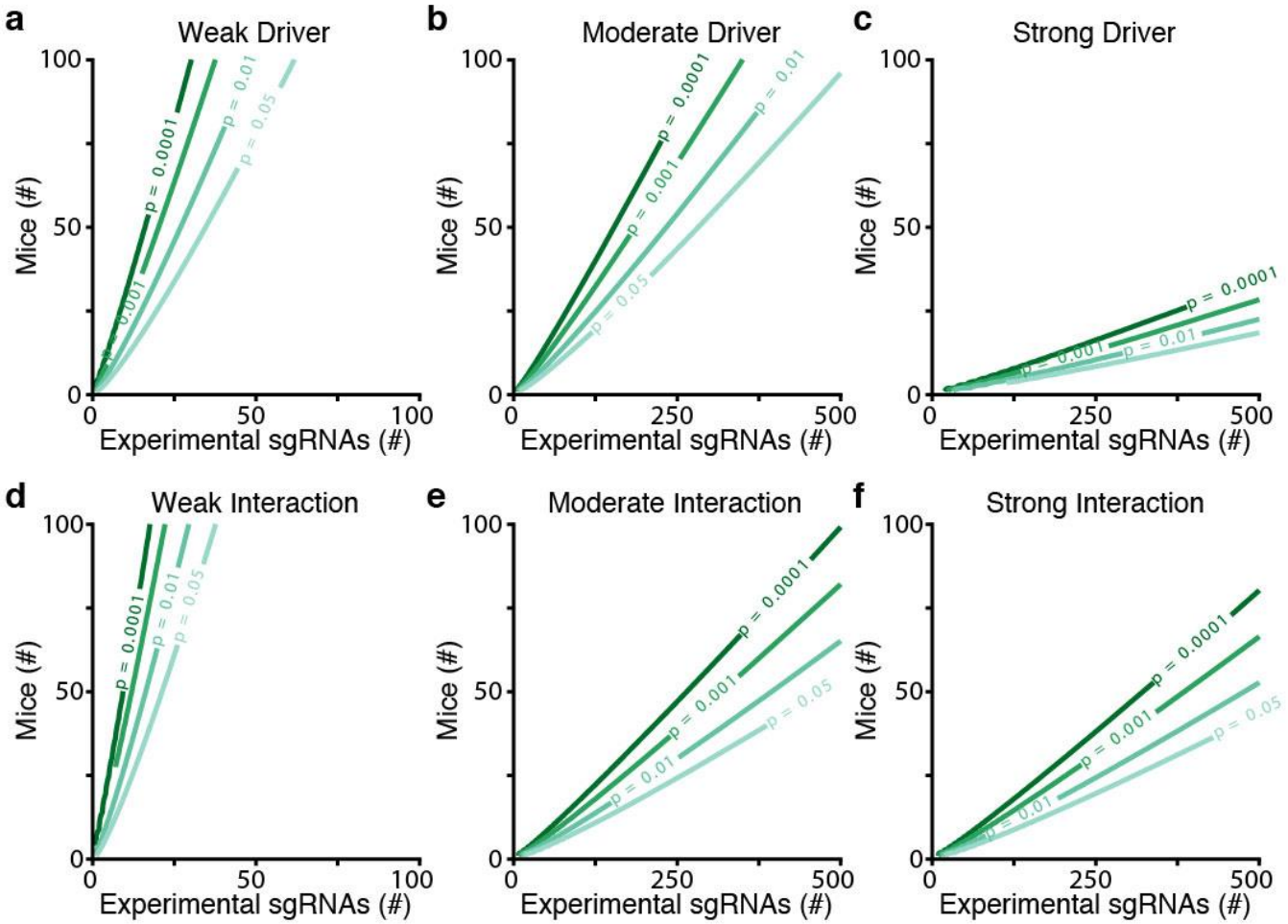

Supplementary Figure 8

Power analysis of larger genetic surveys.

By assuming lognormal tumor size distributions, the statistical power of Tuba-seq to detect driver growth effects and non-additive driver interactions in larger genetic surveys can be projected. Future experiments could utilize larger mouse cohorts and larger pools of sgRNAs targeting putative tumor suppressors. In all hypothetical experiments, the Lenti-sg*TS-Pool/Cre* titers and fraction of the pool with inert sgRNAs (for normalization) were kept consistent with our original experiments.

a. *P*-value contours for the confidence in detecting a weak driver (parameterized by the sg*Cdkn2a* distribution in *KT;Cas9* mice). Any experimental setups above a contour detects weak drivers with a confidence greater than or equal to the *P*-value of the contour.

b,c. Same as in **a**, except for moderate and strong drivers respectively (parameterized by sg*Rb1* and sg*Lkb1* in *KT;Cas9* mice). sgRNA pool size is extended to 500 targets (instead of 100 targets in a pool) because larger screens are possible when investigating genes with these effect strengths.

d-f. Same as in **a-c**, except for driver interactions. Driver interactions (LN Mean Ratio) are defined as a ratio of driver growth rates (sg*TS*/sg*Inert* in background #1)/(sg*TS*/sg*Inert* in background #2) that were statistically different from the null hypothesis of one. (**d**) A weak driver interaction parameterized by *Rbm10—p53* (7% effect size). (**e**) A moderate driver interaction parameterized by *Rb1—p53* (13% effect size). (**f**) A strong driver interaction parameterized by *Setd2—Lkb1* (68% effect size).